Maximizing the Cutoff Rate in a Quantized MIMO Wireless System with AGC

Boyd M. Murray, *Member, IEEE*
CSIRO ICT Centre, Sydney, Australia
University of Technology Sydney, Sydney, Australia
E-mail: Boyd.Murray@csiro.au

Sam Reisenfeld, *Senior Member, IEEE*
University of Technology Sydney, Sydney, Australia
E-mail: Sam.Reisenfeld@uts.edu.au

***Abstract*—**
We investigate the effects of quantization and AGC (Automatic Gain Control) in MIMO (Multiple Input Multiple Output) wireless systems. We derive the cutoff rate equations for a deterministic MIMO channel with quantization at the receiver inputs and demonstrate by numerical simulation the dependence of the cutoff rate on the receiver AGC settings. Then we propose a fast AGC algorithm to maximize the cutoff rate for each channel realization and use it in numerical simulations to evaluate the quantized MIMO system performance in a Rayleigh channel. We find that even quite low resolution quantizers yield cutoff rates very close to those of equivalent unquantized systems when the fast AGC algorithm is applied. Results are presented for BPSK and QPSK modulations for a 2×2 MIMO configuration in deterministic and Rayleigh channels.

I. INTRODUCTION

It is now well known [1], [2] that MIMO wireless systems can be used to achieve high bandwidth efficiencies by using spatial multiplexing to transmit multiple data streams simultaneously within the same frequency spectrum. The cutoff rate [3] is an important tool for evaluating the effect of the modulator/demodulator sub-system on the error performance of coded communication systems. Practical wireless systems use quantizers to convert received analog signals into digital signals for subsequent processing and AGC to minimize the effect of quantization errors. Various studies [4], [5], [6] have evaluated the cutoff rate in unquantized MIMO systems but not in quantized systems. Other studies [3], [7] have optimized the cutoff rate in quantized SISO (Single Input Single Output) systems but not in MIMO systems. The practical effects of quantization and AGC in MIMO sytems have been largely ignored to date. Here, we extend the previous work to use AGC to maximize the cutoff rate of a quantized MIMO system.

We start by deriving the equations for the cutoff rate of a general quantized MIMO system assuming perfect channel state information (CSI) at the receiver. These equations are used to determine the effect of varying the quantizer step size at each receiver on the cutoff rate for a deterministic channel. This is done for a range of quantizer resolutions (quantizer bits). A fast (sub-optimal) AGC algorithm is proposed and then applied to each realization of a MIMO Rayleigh channel. We show that surprisingly low resolution quantizers can achieve close to the cutoff rate of an unquantized system.

II. SYSTEM DESCRIPTION

Consider the quantized MIMO system as shown in Fig. 1. This leads to the system equation

$$\mathbf{q} = \Phi(\mathbf{y}) = \Phi(\mathbf{r}+\mathbf{n}) = \Phi(\mathbf{H}\mathbf{x}+\mathbf{n}) \tag{1}$$

where $\mathbf{q} \in \mathcal{C}^{N_r \times 1}$ is the quantized output, $\Phi(\cdot)$ indicates the quantization operation, $\mathbf{y} \in \mathcal{C}^{N_r \times 1}$ is the unquantized output (with noise), $\mathbf{r} \in \mathcal{C}^{N_r \times 1}$ is the unquantized output at the receiver antennas (before noise), $\mathbf{n} \in \mathcal{C}^{N_r \times 1}$ is i.i.d. zero-mean complex circular Gaussian noise with covariance matrix $E[\mathbf{n}\mathbf{n}^H] = \frac{1}{\gamma}\mathbf{I}_{N_r}$, $\mathbf{H} \in \mathcal{C}^{N_r \times N_t}$ is the channel matrix with entries $h_{i,j}$ representing the channel gain from the j'th transmitter to the i'th receiver, and $\mathbf{x} \in \mathcal{C}^{N_t \times 1}$ is the transmitted symbol (containing BPSK or QPSK symbols) with covariance matrix $E[\mathbf{x}\mathbf{x}^H] = \frac{1}{N_t}\mathbf{I}_{N_t}$. Also, $(\cdot)^H$ indicates Hermitian transpose and the signal to noise ratio (SNR) is defined to be γ.

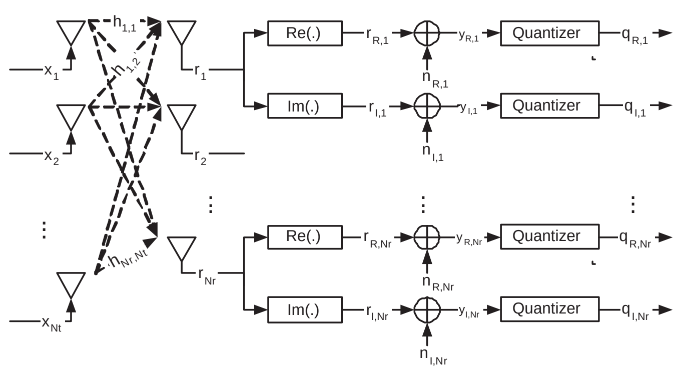

Fig. 1. MIMO system with quantization

III. QUANTIZER DESCRIPTION

As shown in Fig. 1, the real and imaginary components of the signal are each sampled with a finite resolution scalar quantizer which we choose to be a uniform symmetric mid-riser type [8]. The quantizer for complex dimension $c \in \{R, I\}$, where R indicates real and I indicates imaginary, of receiver i will now be described. The quantizer cell boundaries are given by

$$u_{c,i,\ell_{c,i}} = \begin{cases} -\infty \ , & \ell_{c,i} = 1 \\ (\frac{-L}{2} - 1 + \ell_{c,i})\Delta_i \ , & \ell_{c,i} = 2, 3, \cdots, L \\ +\infty \ , & \ell_{c,i} = L + 1 \end{cases} \quad (2)$$

where Δ_i is the quantizer step-size (set the same for the real and imaginary dimensions) and $L = 2^b$ is the number of quantizer levels for b quantizer bits (set the same for all the quantizers). The quantizer input clip level is the same for both real and imaginary dimensions and is given by

$$k_i = -u_{c,i,2} = u_{c,i,L} = (\frac{L}{2} - 1)\Delta_i \ , c \in \{R, I\}. \quad (3)$$

The quantizer output levels are given by

$$v_{c,i,\ell_{c,i}} = (\frac{-L}{2} - \frac{1}{2} + \ell_{c,i})\Delta_i \ , \ \ell_{c,i} = 1, 2, \cdots, L. \quad (4)$$

The quantization function is then given by

$$q_{c,i} = v_{c,i,\ell_{c,i}} \quad , \ u_{c,i,\ell_{c,i}} \leq y_{c,i} < u_{c,i,\ell_{c,i}+1} \ , \ \ell_{c,i} = 1, 2, \cdots, L \quad (5)$$

which is depicted in Fig. 2.

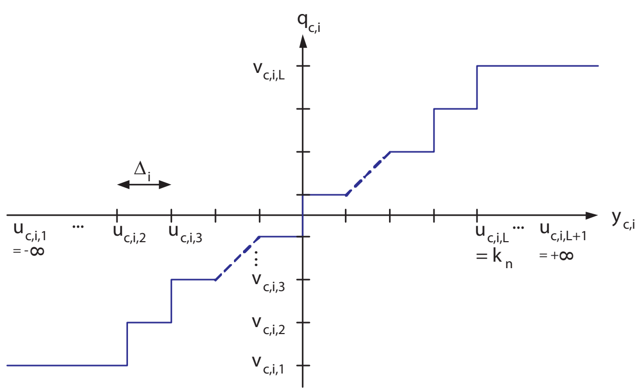

Fig. 2. Quantizer characteristic for complex dimension c of receiver i

IV. CUTOFF RATE

The cutoff rate R_0 can be used for practical finite length block codes in discrete memoryless channels to upper-bound codeword error rates after maximum likelihood decoding according to [3]

$$P_e \leq 2^{-N(R_0 - R)} \ , \ R < R_0 \quad (6)$$

where N is the block length and $R = \frac{k}{n}\log_2(Z)$ is the binary code rate for a $(n,k)_Z$ block code which is defined to have n information bits per block, k coded bits per block and $\log_2(Z)$ code bits per channel symbol (letter) yielding a channel symbol alphabet of size Z. The cutoff rate is a function of the modem implementation which should be designed to maximize it. By rearranging (6), the cutoff rate can be used to set the operating code rate according to

$$R \leq R_0 + \frac{1}{N}\log_2([P_e]_{desired}) < R_0 \quad (7)$$

or to set the code block length according to

$$N \geq \frac{\log_2([P_e]_{desired})}{R - R_0} \ , \ R < R_0. \quad (8)$$

We assume a discrete memoryless channel so that the cutoff rate evaluated at the quantized output $\mathbf{q}$ of the system shown in Fig. 1 is given by [3]

$$R_0 = -\log_2 \sum_{\mathbf{q} \in \mathcal{Q}} \left(\sum_{\mathbf{x} \in \mathcal{X}} P(\mathbf{x}) \sqrt{P(\mathbf{q}|\mathbf{x})} \right)^2 \quad (9)$$

where $\mathcal{Q} = \{\mathbf{q}_1, \mathbf{q}_2, \ldots, \mathbf{q}_Z\}$ is the set of quantized receive symbols (quantized receive alphabet), $\mathcal{X} = \{\mathbf{x}_1, \mathbf{x}_2, \ldots, \mathbf{x}_T\}$ is the set of source symbols (source alphabet), $P(\mathbf{x})$ is the a priori probability of source symbol $\mathbf{x}$, and $P(\mathbf{q}|\mathbf{x})$ is the probability of the quantized received symbol $\mathbf{q}$ conditioned on the source symbol $\mathbf{x}$. We assume each entry x_j (corresponding to transmitter j) of a source symbol $\mathbf{x}$ is drawn from the same discrete BPSK or QPSK modulation alphabet $\mathcal{X}'$, with $|\mathcal{X}'| = M$, so that the source alphabet $\mathcal{X} = \mathcal{X}' \times \mathcal{X}' \times \cdots \times \mathcal{X}'$ is the N_t-factor Cartesian product of each transmitter's source alphabet; and

$$|\mathcal{X}| = T = M^{N_t}. \quad (10)$$

Also, we assume the source symbols are equi-probable so that $P(\mathbf{x}) = \frac{1}{T}$. From (4), the quantized receive alphabet for the quantizer at complex dimension c of receiver i is $\mathcal{Q}_{c,i} = \{v_{c,i,1}, \ v_{c,i,2}, \ \ldots \ , v_{c,i,L}\}$ and $|\mathcal{Q}_{c,i}| = L$. The quantized receive alphabet $\mathcal{Q} = \mathcal{Q}_{R,1} \times \mathcal{Q}_{I,1} \times \mathcal{Q}_{R,2} \times \mathcal{Q}_{I,2} \times \cdots \times \mathcal{Q}_{R,N_r} \times \mathcal{Q}_{I,N_r}$ is the $2N_r$-factor Cartesian product of each quantizer's receive alphabet; and $|\mathcal{Q}| = Z = L^{2N_r}$. With some algebraic manipulation and using results from [9], (9) can be re-written as

$$R_0 = -\log_2(T) - \log_2 \left(1 + \frac{2}{T} \sum_{t=1}^{T-1} \sum_{t'=t+1}^{T} S(t, t') \right) \quad (11)$$

where we define

$$S(t, t') \triangleq \sum_{z=1}^{Z} \sqrt{P(\mathbf{q}_z|\mathbf{x}_t) P(\mathbf{q}_z|\mathbf{x}_{t'})} \quad (12)$$

as the similarity measure for transmitted symbols $\mathbf{x}_t$ and $\mathbf{x}_t'$. Because all of the real and imaginary components of the receiver noise $\mathbf{n}$ are statistically independent, we can express each of the conditional probabilities of (12) as the product of the conditional probabilities on each receiver dimension

$$P(\mathbf{q}|\mathbf{x}) = \prod_{c \in \{R,I\}} \prod_{i=1}^{N_r} P(q_{c,i}|\mathbf{x}) \quad (13)$$

and (12) can then be rewritten as

$$S(t, t') = \sum_{\ell_{R,1}=1}^{L} \sum_{\ell_{I,1}=1}^{L} \cdots \sum_{\ell_{R,N_r}=1}^{L} \sum_{\ell_{I,N_r}=1}^{L} \prod_{c \in \{R,I\}} \prod_{i=1}^{N_r} \sqrt{P(v_{c,i,\ell_{c,i}}|\mathbf{x}_t) P(v_{c,i,\ell_{c,i}}|\mathbf{x}_t')} \quad (14)$$

where the probability of the $\ell_{c,i}$'th quantizer output level on complex dimension c of receiver i conditioned on source symbol $\mathbf{x}$ is

$$P(v_{c,i,\ell_{c,i}}|\mathbf{x}) = Q\left(\frac{u_{c,i,\ell_{c,i}} - [\mathbf{Hx}]_{c,i}}{\sigma_{c,i}}\right) - Q\left(\frac{u_{c,i,\ell_{c,i}+1} - [\mathbf{Hx}]_{c,i}}{\sigma_{c,i}}\right) \quad (15)$$

where $Q(x) = \int_x^\infty e^{\frac{-t^2}{2}} dt$ is the complementary cumulative distribution function and

$$\sigma_{c,i} = \frac{1}{\sqrt{2\gamma}} \quad (16)$$

is the standard deviation of the noise at each quantizer input. The cutoff rate R_0 of the quantized system can now be evaluated by substituting (2), (3), (10), (14), (15), and (16) into (11). We note in particular that R_0 is a function of the modulation alphabet at each transmitter $\mathcal{X}'$, the vector of quantizer step-sizes at each receiver $\mathbf{\Delta} = [\Delta_1\ \Delta_2\ \ldots\ \Delta_{N_r}]$, the number of quantizer bits b, the channel $\mathbf{H}$, and the SNR γ.

For comparison, the cutoff rate of an unquantized (infinite resolution) system is [9]

$$R_0 = -\log_2(T) -\log_2\left(1 + \frac{2}{T}\sum_{t=1}^{T-1}\sum_{t'=t+1}^{T} \exp\left(-\frac{||\mathbf{Hx}_t - \mathbf{Hx}'_t||^2}{4\sigma_n^2}\right)\right) \quad (17)$$

where $\sigma_n = \frac{1}{\sqrt{\gamma}}$ is the standard deviation of the noise at each receiver.

V. CUTOFF RATE EXAMPLE FOR A FIXED MIMO CHANNEL

We use AGC to maximize the cutoff rate R_0 for each channel $\mathbf{H}$ in order to minimize the upper bound on the codeword error rate according to (6). We define the normalized quantizer clip level at receiver i to be

$$\kappa_i = \frac{k_i}{\max(\max_{\mathbf{x}\in\mathcal{X}}([\mathbf{Hx}]_{R,i}), \max_{\mathbf{x}\in\mathcal{X}}([\mathbf{Hx}]_{I,i}))}. \quad (18)$$

That is, κ_i is the quantizer clip level k_i normalized to the maximum of the real and imaginary components of all the received constellation points at receiver i. The AGC function is implemented by setting the vector of normalized quantizer clip levels $\kappa = [\kappa_1\ \kappa_2\ \ldots\ \kappa_{Nr}]$ to achieve maximal cutoff rate R_0. Note that κ is related to the vector of quantizer stepsizes Δ through (18) and (3).

Fig. 3 shows simulation results for a 2×2 QPSK MIMO system with 2 quantization bits and a fixed channel $\mathbf{H}$. Note that R_0^b indicates the cutoff rate when all quantizers use b bits and R_0^∞ indicates the cutoff rate for an unquantized (infinite resolution) system. The received signal constellations (before noise) are shown in Fig. 3(a) and (b). The dependence of the cutoff rate R_0^2 on the normalized clip levels κ is shown in Fig. 3(c) to (k). For low SNRs (γ = 0dB), R_0^2 is quite tolerant to variations in κ as seen in Fig. 3(c), (f), and (i). For intermediate SNRs (γ = 15dB), a clear optimum occurs as seen in Fig. 3(d), (g), and (j). For high SNRs (γ = 30dB), R_0^2 is again quite tolerant to variations in κ about the optimum as seen in Fig. 3(e), (h), and (k). At each simulated SNR, the vector of optimal normalized clip levels $\kappa_{opt} = [\kappa_{opt,1}\ \kappa_{opt,2}]$ was found by a rigorous search and is shown in Fig. 3(l). The corresponding optimal cutoff rate $R_{0,opt}^2$ is shown in Fig. 3(m) together with the cutoff rate R_0^∞ for infinite resolution quantization and the cutoff rate $R_{0,set}^2$ for a fixed setting of the normalized clip levels $\kappa_{set} = [0.7\ 0.5]$. κ_{set} was chosen to optimize R_0^2 at γ =15dB which yields very close to optimal cutoff rates over the entire range of γ as evidenced by the close overlap of the $R_{0,opt}$ and $R_{0,set}^2$ curves in Fig. 3(l). κ_{set} is indicated by dotted lines in Fig. 3(c) to (k) and the quantizer cell boundaries corresponding to κ_{set} are indicated by dotted lines in Fig. 3(a) and (b). The results shown in Fig. 3 were for a particular channel $\mathbf{H}$ which was chosen to demonstrate a cutoff rate which is highly sensitive to κ. Generally, each different combination of the modulation order M, quantizer bits b, and the channel $\mathbf{H}$ yields different results for which, in most cases, R_0 is not as sensitive to κ as in Fig. 3.

VI. FAST AGC ALGORITHM

The simulations of Fig. 3 required a 2-dimensional search over κ_1 and κ_2 to find the optimal R_0 for every SNR. Additional simulations showed that a fast AGC algorithm yielded close to optimal cutoff rate over the entire SNR range for numerous simulated Rayleigh channel realizations. The fast AGC algorithm consists of two 1-dimensional searches and is described as follows. a) Set γ = 15dB, b) set $\kappa_1 = 1$, c) search for optimal (maximal) R_0 while varying κ_2 over range 0 to 4, d) set κ_2 to its optimum value, e) search for optimal (maximal) R_0 while varying κ_1 over range 0 to 4, f) set κ_{set} with the optimal values of κ_1 and κ_2, and g) use κ_{set} to calculate R_0 at all SNRs. This fast AGC algorithm assumes perfect CSI at the receiver which is used in the calculations to optimize the cutoff rate R_0 for each channel $\mathbf{H}$.

VII. QUANTIZED RECEIVER PERFORMANCE WITH AGC IN RAYLEIGH CHANNEL

We now evaluate the performance of the quantized system with AGC in a flat-fading Rayleigh channel $\mathbf{H}$ with i.i.d. zero-mean unit variance complex circular Gaussian elements. We assume block-fading where each channel realization is independent of all other realizations. For each channel realization, the fast AGC algorithm described above is applied to select the AGC to achieve close to the optimal cutoff rate. The cutoff rate for the quantized system with AGC in the Rayleigh channel is formulated by using the expectation of the similarity measure over the Rayleigh channel [5] and is given by

$$R_0 = -\log_2(T) - \log_2\left(1 + \frac{2}{T}\sum_{t=1}^{T-1}\sum_{t'=t+1}^{T} E_{\mathbf{H}}\{S(t,t')\}\right) \quad (19)$$

where $E_{\mathbf{H}}\{\cdot\}$ indicates the expectation over the channel $\mathbf{H}$ and $S(t,t')$ is evaluated for each channel realization after applying

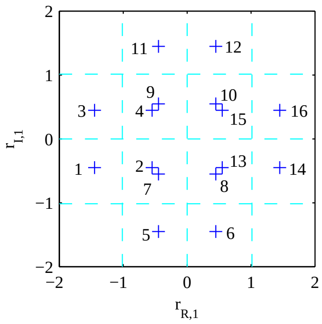

(a) Constellation at receiver 1.

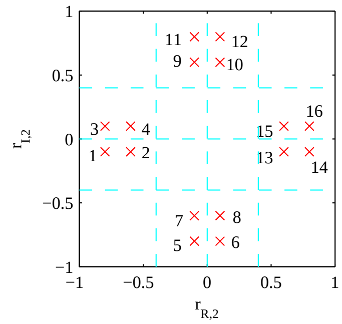

(b) Constellation at receiver 2.

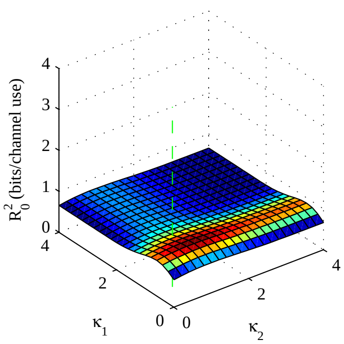

(c) R_0^2 vs κ_1, κ_2 with $\gamma = 0$dB.

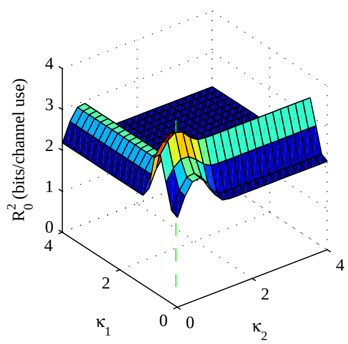

(d) R_0^2 vs κ_1, κ_2 with $\gamma = 15$dB.

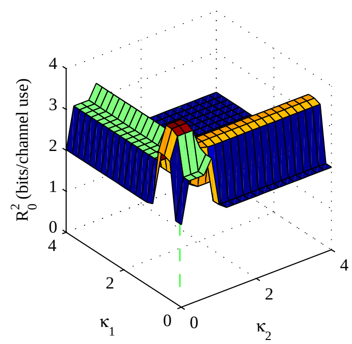

(e) R_0^2 vs κ_1, κ_2 with $\gamma = 30$dB.

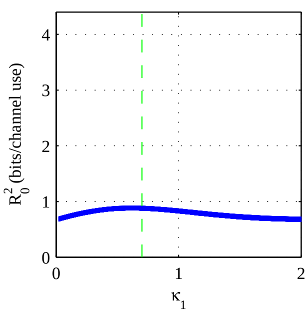

(f) R_0^2 vs κ_1 with $\kappa_2 = 0$ to $4, \gamma = 0$dB.

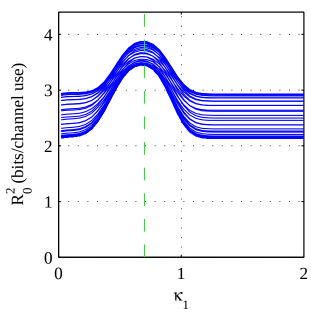

(g) R_0^2 vs κ_1 with $\kappa_2 = 0$ to $4, \gamma = 15$dB.

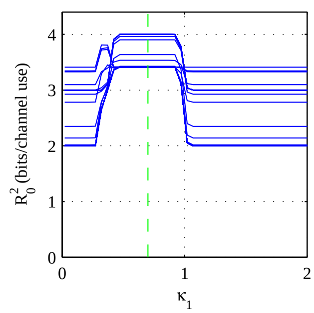

(h) R_0^2 vs κ_1 with $\kappa_2 = 0$ to $4, \gamma = 30$dB.

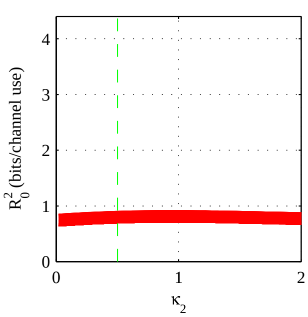

(i) R_0^2 vs κ_2 with $\kappa_1 = 0$ to $4, \gamma = 0$dB.

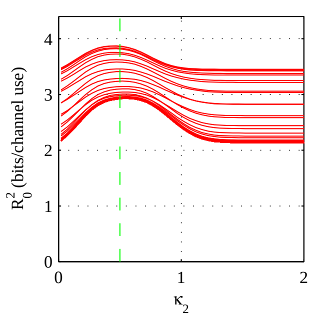

(j) R_0^2 vs κ_2 with $\kappa_1 = 0$ to $4, \gamma = 15$dB.

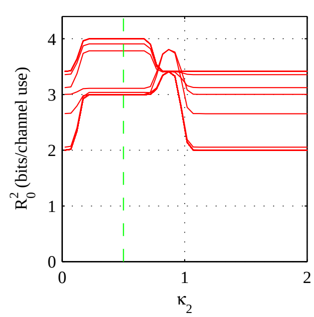

(k) R_0^2 vs κ_2 with $\kappa_1 = 0$ to $4, \gamma = 30$dB.

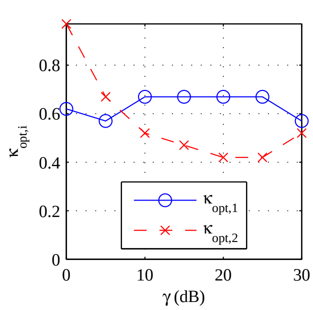

(l) Optimal normalized clip levels

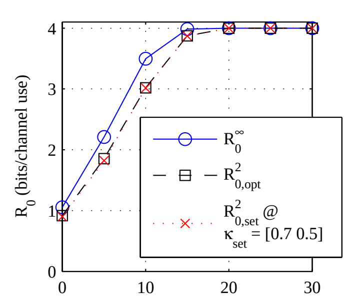

(m) Cutoff rates

Fig. 3. Simulation results for $N_t = 2$, $N_r = 2$, $M = 4$ (QPSK), $b = 2$, and $\mathbf{H} = [1.0 + 1.0\mathrm{i}\ 0.0 + 0.9\mathrm{i}; 0.7 + 0.7\mathrm{i}\ 0.0 + 0.2\mathrm{i}]$.

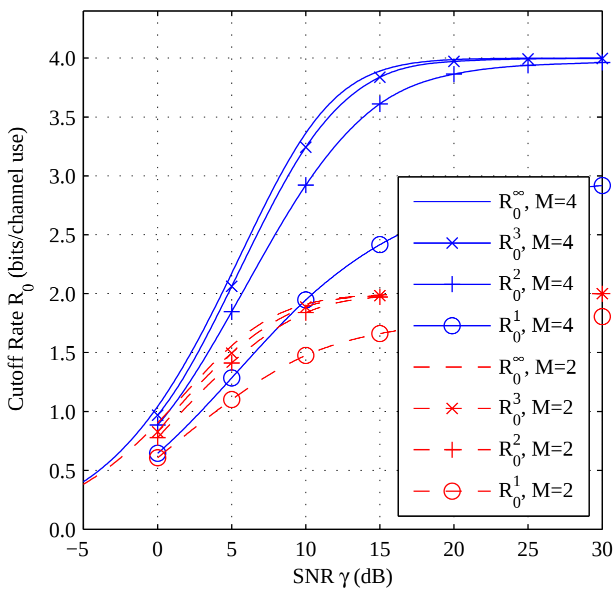

Fig. 4. Cutoff rates in a Rayleigh 2×2 MIMO channel with AGC for BPSK ($M = 2$) and QPSK ($M = 4$) and quantizer bits $b = 1, 2, 3$, and ∞.

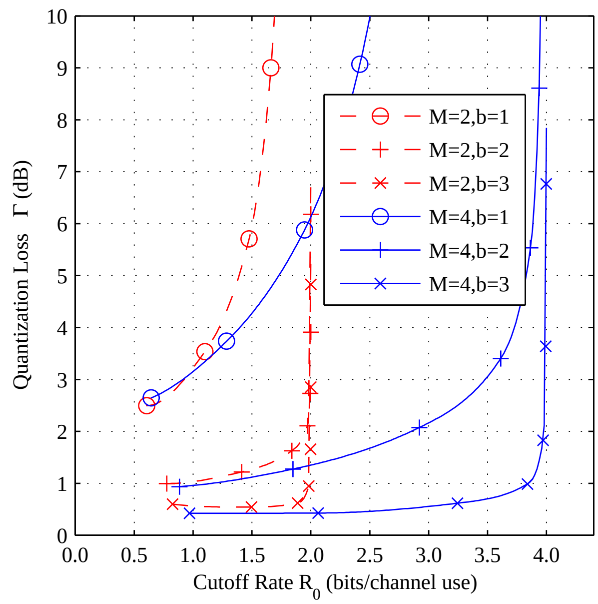

Fig. 5. Quantization loss in a Rayleigh 2×2 MIMO channel with AGC for BPSK ($M = 2$) and QPSK ($M = 4$) and quantizer bits $b = 1, 2$ and 3.

the fast AGC algorithm. We note that R_0 is a function of the modulation alphabet at each transmitter $\mathcal{X}'$ (also described by the modulation order M), the number of quantizer bits b, and the SNR γ. In our simulations, $E_{\mathbf{H}}\{S(t,t')\}$ is numerically approximated by averaging $S(t,t')$ over a sufficiently large number of randomly selected Rayleigh channel realizations. The cutoff rate simulation results are shown in Fig. 4.

The quantization loss under the cutoff rate criterion for b bits is

$$\Gamma(R) = \frac{\gamma_{|R_0^\infty = R}}{\gamma_{|R_0^b = R}}. \tag{20}$$

The simulation results of Fig. 5 show that quantization losses of less than 0.6dB can be achieved over a large range of cutoff rates for only $b = 3$ quantizer bits for both BPSK ($M = 2$) and QPSK ($M = 4$) modulations. For $b = 2$ quantizer bits, the quantization loss is higher at around 1dB for low cutoff rates and rises quicker than for $b = 3$ as the cutoff rate rises for both BPSK and QPSK.

VIII. CONCLUSIONS

This paper has examined the performance of practical MIMO implementations with quantization and AGC. Assuming perfect CSI at the receiver, we have derived the cutoff rate for the quantized system and used simulations to show the dependence of the cutoff rate on the normalized clip levels of the quantizers. Also, we have shown that, by using a straightforward fast AGC algorithm, quantization losses of less than 0.6dB under the cutoff rate criterion can be achieved using only 3 quantizer bits for BPSK and QPSK modulations with a 2×2 MIMO configuration in a Rayleigh channel.

REFERENCES

[1] J. H. Winters, “On the capacity of radio communication systems with diversity in a rayleigh fading environment,” *IEEE J. Select. Areas Commun.*, vol. SAC-5, no. 5, pp. 871–878, Jun. 1987.

[2] E. Teletar, “Capacity of multi-antenna Gaussian channels,” *Europ. Trans. Commun.*, pp. 585–595, Nov.-Dec. 1999.

[3] J. L. Massey, “Coding and modulation in digital communications,” Mar. 1974, presented at the Int. Zurich Seminar, Sindelfingen, Germany.

[4] A. O. Hero and T. L. Marzetta, “On computational cut-off rate for space-time coding,” Bell Laboratories, Lucent Technologies, Murray Hill, NJ, Tech. Rep., 1999.

[5] ——, “Optimal signal constellations for space-time rayleigh channels,” Bell Laboratories, Lucent Technologies, Murray Hill, NJ, Tech. Rep., 1999.

[6] M. T. Ivrlac, W. Utschick, and J. Nossek, “Fading correlations in wireless MIMO communication systems,” *IEEE J. Select. Areas Commun.*, vol. 21, no. 5, pp. 819–828, Jun. 2003.

[7] S. Baggen, S. Egner, and B. Vandewiele, “Using R_0 for determining the quantization of the input of a viterbi decoder on fading channels,” Philips Research Laboratories, Prof. Holstlaan 4, 5656 AA Eindhoven, The Netherlands, Tech. Rep., May. 2003.

[8] A. Gersho and R. M. Gray, *Vector Quantization and Signal Compression*. Kluwer Academic Publishers, 1992.

[9] T. Kurpjuhn and M. Ivrlac, “Information theoretic measures for MIMO-channels,” Lehrstuhl für Netzwertheorie und Signalvararbeitung, Munich, Germany, Technische Univ. München, Tech. Rep. TUM-LNS-TR-01-01, 2001.